The Astrophysical Journal, 691:L27–L32, 2009 January 20 doi:10.1088/0004-637X/691/1/L27

THE FIRST POSITIVE DETECTION OF MOLECULAR GAS IN A GRB HOST GALAXY

J. X. Prochaska[1,2], Y. Sheffer[3], D. A. Perley[4], J. S. Bloom[4,8], L. A. Lopez[2], M. Dessauges-Zavadsky[5], H.-W. Chen[6], A. V. Filippenko[4], M. Ganeshalingam[4], W. Li[4], A. A. Miller[4], and D. Starr[4,7]
[1] University of California Observatories/Lick Observatory, University of California, Santa Cruz, CA 95064, USA
[2] Department of Astronomy and Astrophysics, University of California, Santa Cruz, CA 95064, USA
[3] Department of Physics and Astronomy, University of Toledo, Toledo, OH 43606, USA
[4] Department of Astronomy, University of California, Berkeley, CA 94720-3411, USA
[5] Observatoire de Genève, 51 Ch. des Maillettes, 1290 Sauverny, Switzerland
[6] Department of Astronomy & Astrophysics, and Kavli Institute for Cosmological Physics, 5640 S. Ellis Ave, Chicago, IL 60637, USA
[7] Las Cumbres Observatory, 6740 Cortona Dr. Suite 102, Santa Barbara, CA 93117, USA
Received 2008 October 27; accepted 2008 December 3; published 2008 December 29

ABSTRACT

We report on strong H_2 and CO absorption from gas within the host galaxy of gamma-ray burst (GRB) 080607. Analysis of our Keck/LRIS afterglow spectrum reveals a very large H I column density ($N_{\rm H\,I} = 10^{22.70\pm0.15}\,{\rm cm}^{-2}$) and strong metal-line absorption at $z_{\rm GRB} = 3.0363$ with a roughly solar metallicity. We detect a series of $A-X$ bandheads from CO and estimate $N({\rm CO}) = 10^{16.5\pm0.3}\,{\rm cm}^{-2}$ and $T_{\rm ex}^{\rm CO} > 100\,{\rm K}$. We argue that the high excitation temperature results from UV pumping of the CO gas by the GRB afterglow. Similarly, we observe H_2 absorption via the Lyman–Werner bands and estimate $N_{H_2} = 10^{21.2\pm0.2}\,{\rm cm}^{-2}$ with $T_{\rm ex}^{H_2} = 10$–$300\,{\rm K}$. The afterglow photometry suggests an extinction law with $R_V \approx 4$ and $A_V \approx 3.2$ mag and requires the presence of a modest 2175 Å bump. Additionally, modeling of the *Swift* XRT X-ray spectrum confirms a large column density with $N_{\rm H} = 10^{22.58\pm0.04}\,{\rm cm}^{-2}$. Remarkably, this molecular gas has extinction properties, metallicity, and a CO/H_2 ratio comparable to those of translucent molecular clouds of the Milky Way, suggesting that star formation at high z proceeds in similar environments as today. However, the integrated dust-to-metals ratio is sub-Galactic, suggesting the dust is primarily associated with the molecular phase while the atomic gas has a much lower dust-to-gas ratio. Sightlines like GRB 080607 serve as powerful probes of nucleosynthesis and star-forming regions in the young universe and contribute to the population of "dark" GRB afterglows.

Key words: gamma rays: bursts – ISM: molecules

Online-only material: machine-readable table

1. INTRODUCTION

Most long-duration, soft-spectrum gamma-ray bursts (GRBs) are thought to arise in the death of massive stars (see Woosley & Bloom 2006 for a review). The evidence for this is both direct, such as the observation of a contemporaneous supernova associated with some events (e.g., Stanek et al. 2003; Hjorth et al. 2003), and circumstantial, based on physical associations with star-forming galaxies (see Fruchter et al. 2006). Still, some telltale signatures of massive-star progenitors are rarely, if ever, observed. The absence of wind-blown density profiles in the circumburst environment (Chevalier 2004) is thought to be due to the pre-burst interactions of the wind with the interstellar medium (ISM; Ramirez-Ruiz et al. 2005). The absence of Wolf–Rayet signatures in afterglow spectra (Chen et al. 2007) is explained by the influence of the afterglow light on gas and dust within ~ 100 pc of the GRB event.

Outside the overwhelmingly destructive influence within the inner 100 pc, there are generic signatures of the ISM: H I gas ($\Sigma_{\rm H\,I} \approx 1$–$100\ M_\odot\ {\rm pc}^{-2}$; Jakobsson et al. 2006), metal-enriched material (Savaglio et al. 2003), and large depletion factors indicating significant dust formation (e.g., Watson et al. 2006; Prochaska et al. 2007). Indirectly, one also infers significant extinction from the reddening of some afterglows (e.g., Watson et al. 2006; Elíasdóttir et al. 2008) and from the large metal column densities implied by absorption of the X-ray afterglow (e.g., Galama & Wijers 2001; Campana et al. 2006; Butler & Kocevski 2007).

Evidence for molecular gas, a crucial ingredient of star formation, has proved elusive thus far. Tumlinson et al. (2007) presented a survey for H_2 Lyman–Werner absorption in the afterglow spectra of four GRBs and reported no positive detections. Fynbo et al. (2006) tentatively interpreted an absorption feature in their spectrum of GRB 060206 as H_2, but this may instead be interpreted as an unrelated Lyα absorption line. The absence of molecules local to the GRB progenitor may be explained as a natural consequence of photodissociation by the star prior to its death (Whalen et al. 2008). The absence of molecules along the full sightline, meanwhile, suggests that an elevated UV radiation field is suppressing H_2 formation throughout the host galaxy (Chen et al. 2008). Nevertheless, these galaxies are actively forming stars (Christensen et al. 2004) and GRB sightlines should occasionally penetrate neighboring molecular clouds on the path to Earth.

In this Letter, we present the first such unambiguous detection of H_2 and CO absorption in a GRB host galaxy and provide initial analysis of the gas and dust along the sightline to GRB 080607. Previous detections of intervening CO absorption toward quasars have only shown trace quantities of molecular gas (Srianand et al. 2008). Emission-line studies of CO and other molecules, meanwhile, lack sufficient spatial resolution to resolve the gas beyond the local universe (e.g., Tacconi et al. 2006). Our data constrain the physical conditions of the ISM including its metallicity, dust properties, and molecular fractions. We discuss these results and the prospects for future studies of molecular clouds using GRB afterglows.

[8] Sloan Research Fellow.

2. OBSERVATIONS

We (J.S.B. and D.P.) initiated spectroscopic observations of the GRB 080607 afterglow with Keck I/LRIS (Oke et al. 1995) at 06:27:39 UT on 2008 June 7, ∼ 20 min following the *Swift* trigger of the GRB (Mangano et al. 2008). The Keck/LRIS spectrograph has two cameras optimized for blue (LRISb; $\lambda \approx 3000$–5000 Å) and red (LRISr; $\lambda \approx 5000$–9000 Å) optical wavelengths. Using the 1″ wide long slit, the atmospheric dispersion corrector, and the D560 dichroic, we obtained a series of three two-dimensional spectra of increasing exposure time totaling 2100 s using the B600 grism in LRISb (FWHM $\approx$ 270 km s^{-1}) and the R400 grating in LRISr (FWHM $\approx$ 300 km s^{-1}, centered at $\lambda_{\rm center} \approx 7310$ Å). We then paused to obtain calibration frames before continuing with a sequence of two exposures (1500 s each) with the B600 grism and the R1200 grating (FWHM $\approx$ 110 km s^{-1}, $\lambda_{\rm center} \approx$ 6300 Å). All data were obtained under photometric conditions and a seeing better than 1″. The data were reduced and calibrated using the LowRedux[9] software package developed by S. Burles, J. Hennawi, and J.X.P. using arc images and a spectrum of HZ44.

The Peters Automated Infrared Imaging Telescope (PAIRITEL; Bloom et al. 2006) responded automatically to the *Swift* trigger and began simultaneous observations in the J, H, K_s bands at 06:08:44 UT. A total of 387 individual 7.8 s exposures were taken under moderate conditions, seeing ∼ 3″, for a total time on target of ∼ 3000 s. We have reduced these data with the standard PAIRITEL pipeline. The Katzman Automatic Imaging Telescope (KAIT; Filippenko et al. 2001; Li et al. 2003) also responded to the *Swift* alert of GRB 080607 automatically, and began the first image at 06:09:25 UT, 118 s after the BAT trigger. A series of *V*, *I*, and unfiltered images were obtained for the first ∼ 1800 s after the burst under good conditions.

3. ANALYSIS

In Figure 1 we present the combined LRIS spectra of the GRB afterglow. A very strong absorption feature is evident at $\lambda_{\rm obs} \approx 4900$ Å corresponding to damped Lyα (DLA) absorption from gas within the galaxy hosting GRB 080607. The coincidence of strong metal-line transitions including fine-structure lines of Fe II and Si II confirms this association (Vreeswijk et al. 2004; Prochaska et al. 2006). A Gaussian fit to the strongest low-ion transitions gives a heliocentric redshift $z_{\rm GRB} = 3.0363 \pm 0.0003$.

The dashed curves represent our model for the intrinsic afterglow spectrum, reddened by dust along the sightline. Assuming an intrinsic optical–infrared power-law spectral slope $f_\nu \propto \nu^{-\beta_{\rm O}}$, we first fit the *JHK* photometry for the single parameter $E(B-V) = 0.8 \pm 0.1$ mag. In this analysis we accounted for the uncertainty in the unknown intrinsic spectral index, which for afterglows at early times is found to be in the range $\beta_{\rm O} = 0.1$–1.1 (Kann et al. 2007). We then fitted a Fitzpatrick & Massa (1990) dust model to unabsorbed regions of the R400 spectrum (correcting for Galactic extinction), holding $E(B-V)$ fixed but allowing all other parameters to vary.[10] For an assumed $\beta_{\rm O} = 0.5$, our best-fit parameters are $R_V = 4.0 \pm 0.23$, $A_V = 3.2 \pm 0.5$ mag, $c_3 = 1.3 \pm 0.3$, and $c_4 = 0.3 \pm 0.1$ (Figure 2(a)).

Although there is considerable degeneracy among these values, we reach three robust conclusions: (i) the R_V value is higher than the typical Galactic and SMC values; (ii) the data require a nonzero c_3 parameter indicating the positive detection of the 2175 Å bump, only the second detection of this feature associated with a GRB host galaxy (Krühler et al. 2008; Elíasdóttir et al. 2008); and (iii) the data favor a low c_4 value suggesting few small dust grains. These characteristics are distinguished from the extinction laws commonly inferred for GRB sightlines which generally have SMC-like or "gray" extinction curves and lack evidence for a 2175 Å bump (e.g., Kann et al. 2006; Butler et al. 2006; Watson et al. 2006; Perley et al. 2008).

With the reddened afterglow spectrum as our input continuum, we have fitted the Lyα absorption to the data redward of 5000 Å with centroid $\lambda = 1215.67(1 + z_{\rm GRB})$ Å. The best-fit value for the H I column density is $N_{\rm H\,I} = 10^{22.70\pm0.15}$ cm^{-2}, where the *uncertainty* is dominated by the continuum model. We detect the afterglow down to at least $\lambda \approx 4000$ Å, primarily in a series of emission "gaps" (e.g., at $\lambda_{\rm obs} \approx 4200, 4275, 4315$ Å). Although the absorption between the gaps could be strong intergalactic medium (IGM) absorption, this would require a much higher integrated opacity than observed along quasar sightlines. We interpret the majority of this opacity as Lyman–Werner bands of molecular hydrogen at $z = z_{\rm GRB}$.

The LRISr/R400 spectrum (Figure 1(b)) covers rest wavelengths $\lambda_{\rm rest} > 1300$ Å relative to the GRB and, as such, *none of the absorption* is related to the Lyα forest despite its similar appearance. Instead, the features are metal-line absorption by gas in the GRB host galaxy (Figure 3) and/or intervening gas. We have measured equivalent widths (W_λ) for these features by fitting Gaussian profiles or, in cases of severe line blending, by boxcar summation over the spectral window (Table 1). The absorption is dominated by resonance transitions and fine-structure lines of abundant atoms and ions at $z = z_{\rm GRB}$, but we also identify absorption from two strong Mg II absorbers ($W_{2796} > 1$ Å) at $z = 1.340$ and 1.462, an unusually common characteristic of GRB afterglow spectroscopy (Prochter et al. 2006).

The GRB absorption features are highly saturated and one can only estimate lower limits to the ionic column densities. Under the *very* conservative assumption that $N = 10^{23.05} W_\lambda/(f\lambda^2)$ cm^{-2} (i.e., the weak limit of the curve of growth, with f the oscillator strength), we infer [S/H] > -1.7, [Si/H] > -2, [Fe/H] > -1.8, and [Zn/H] > -1.7. We also detect very weak transitions of several common elements (e.g.,

Table 1
EW Measurements

Region (Å)	λ_c^a (Å)	$W_{\rm obs}$ (Å)	ID	$z_{\rm abs}$
		B600		
[5045.3, 5053.5]		6.73 ± 0.27	S II 1250	3.037
[5055.7, 5065.0]		7.58 ± 0.28	Cr II 2056	1.462
			S II 1253	3.037
[5081.2, 5093.6]		10.66 ± 0.33	Cr II 2066	1.462
			S II 1259	3.037

Note. [a] Central wavelength determined from a Gaussian fit. $W_{\rm obs}$ values determined from boxcar integrations have no value listed.
(This table is available in its entirety in a machine-readable form in the online journal. A portion is shown here for guidance regarding its form and content.)

[9] http://www.ucolick.org/~xavier/LowRedux/index.html
[10] This allows for color evolution between the times of the photometric and spectroscopic observations.

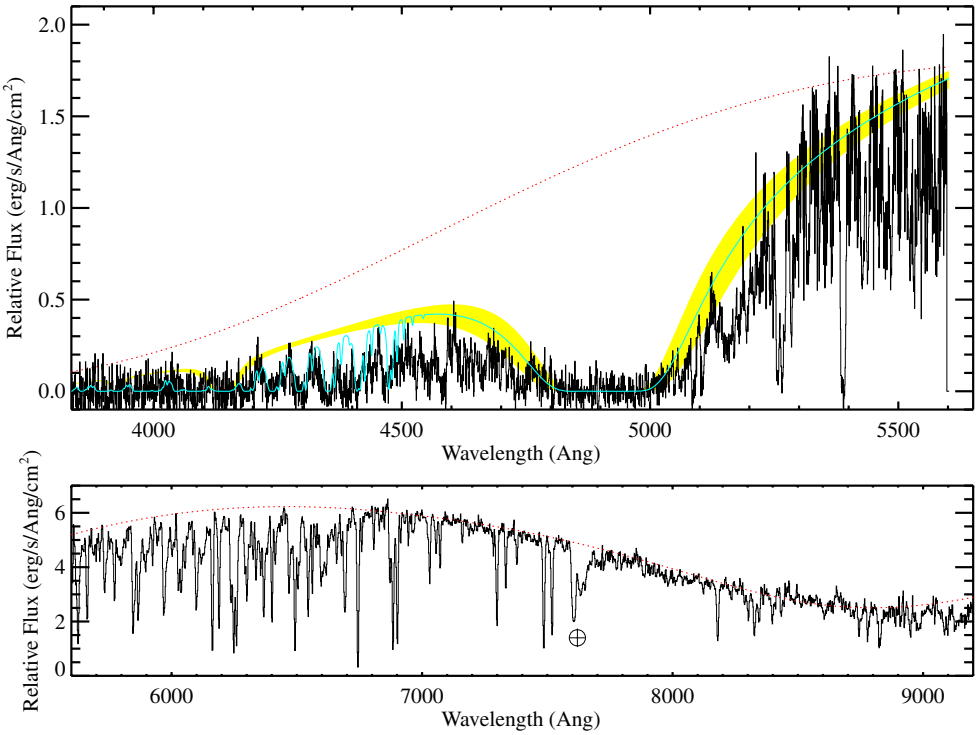

Figure 1. Keck/LRIS spectra of the optical afterglow of GRB 080607 taken with (a) the LRISb camera and the B600 grism and (b) the LRISr camera with the R400 grating. The red dashed lines indicate our model of the intrinsic afterglow spectrum reddened by dust in the host galaxy. At $\lambda \approx 4900$ Å one identifies a DLA profile associated with H I gas near the GRB. The shaded region overplotted on the data corresponds to an H I column density $N_{\rm H\,I} = 10^{22.7\pm0.15}$ cm^{-2}. The model (cyan solid line) includes absorption from H_2 Lyman–Werner transitions. The line opacity at $\lambda > 5500$ Å is dominated by metal-line transitions from gas in the host galaxy and includes bandheads of the CO molecule. Absorption from the Earth's A-band is marked by a $\oplus$.

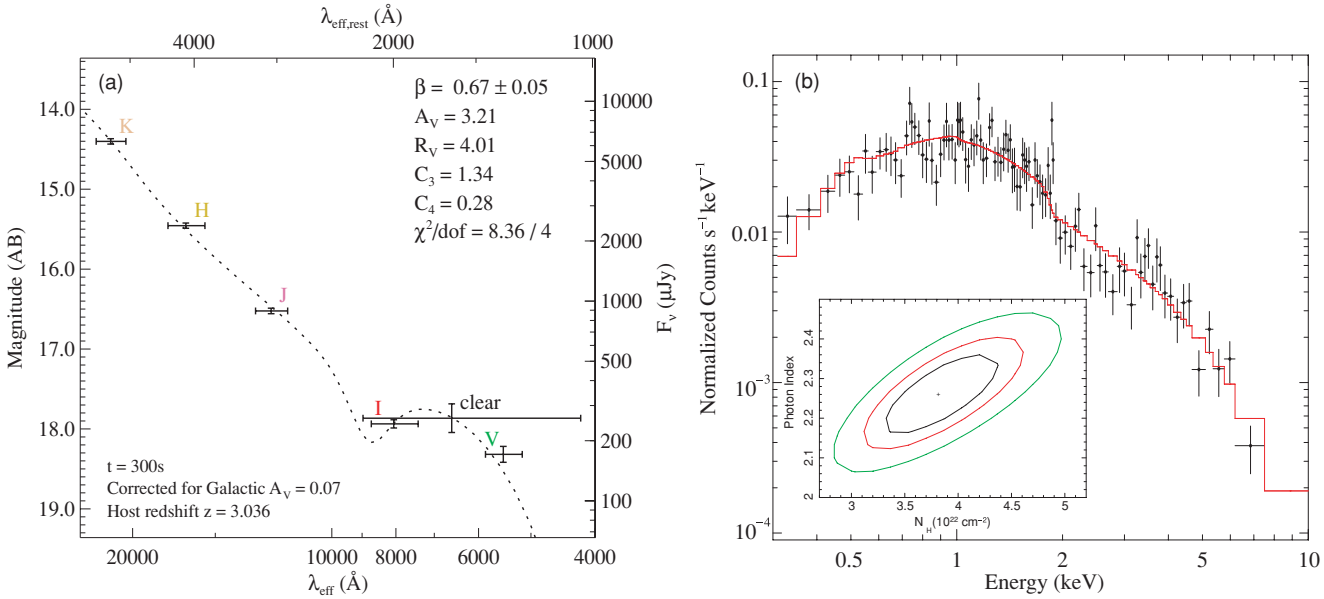

Figure 2. (a) Optical/IR photometry for the afterglow of GRB 080607, as observed by PAIRITEL and KAIT (see Updike et al. in prep.). Overplotted on the data is our best-fit model for an dust-extinguished power-law spectrum, $f_\nu \propto \nu^{-\beta}$. The model, which has a modified Galactic extinction law, must include the 2175 Å feature to match the observations. (b) *Swift* XRT X-ray spectrum (0.3–10.0 keV) obtained 0.6–376 ks after the trigger, with the best-fit model overlaid in red. The data were modeled as a power law, with a Galactic absorption component as well as a redshifted intrinsic absorption component $N_{\rm H}$. The best-fit model has an intrinsic $N_{\rm H} = 10^{22.58\pm0.04}$ cm^{-2} and a photon index 2.26 ± 0.07, using the Galactic absorption 1.9×10^{20} cm^{-2} (Dickey & Lockman 1990). The 68%, 95%, and 99% confidence contours of the photon index and intrinsic absorption are shown.

O I 1355, Ni II 1804, Mg I 1683, Co II 1574) and a few transitions from rare elements (e.g., Ge II 1602). The equivalent width of the Ge II 1602 transition alone implies a lower limit [Ge/H] > 0 and analysis of Co II transitions, a refractory element, yields [Co/H] > -0.7 dex. This is consistent with the equivalent width of the absorption coinciding with the O I 1355 transition which implies [O/H] > -0.2 dex. We conclude that the integrated gas metallicity is solar or even super-solar, a result that challenges the prevailing collapsar model (e.g., Woosley & Heger 2006).

The optical spectra also reveal the positive detection of a series of CO $A-X$ bandheads (Figure 4). It is noteworthy that the peak depth of the bandheads is offset by $\delta v \approx +150$ km s^{-1} from

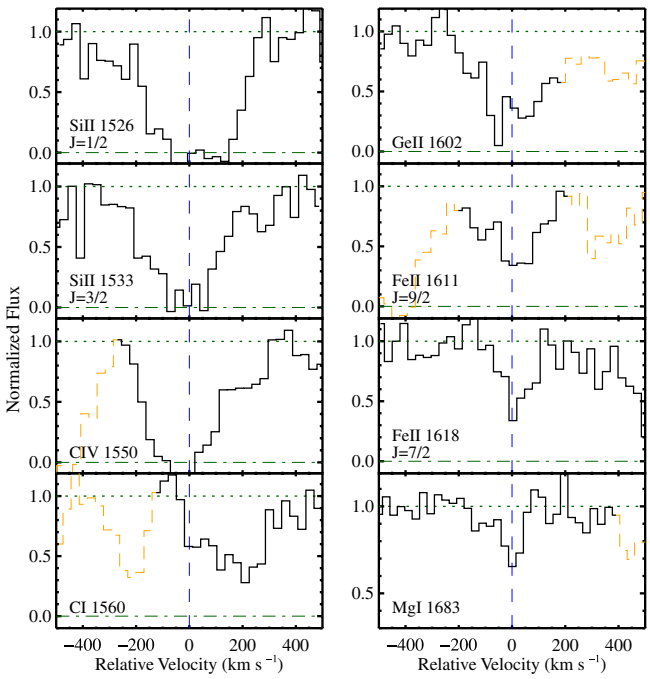

Figure 3. Velocity plots of a subset of the atomic and ionic transitions associated with the ISM of the galaxy hosting GRB 080607. In all panels, $v = 0$ km s^{-1} corresponds to $z_{\rm GRB} = 3.0363$ and the orange dashed lines indicate blends between transitions.

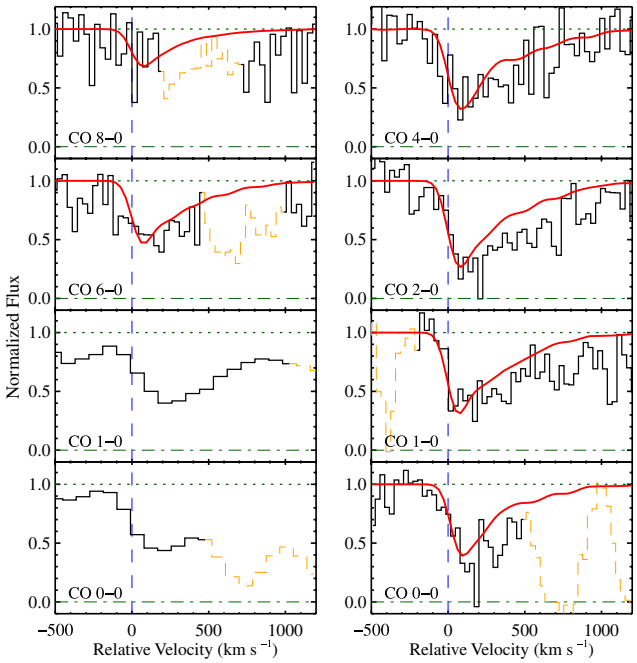

Figure 4. Velocity plots of the molecular transitions associated with the ISM of the galaxy hosting GRB 080607. The first column shows the CO $A - X$ bandheads taken with the LRISb/B600 grism (top two) and LRISr/R400 grating (bottom two). All other data refers to the LRISr/R1200 spectrum. The red line overplotted on the CO data indicate our best-fit model corresponding to $N({\rm CO}) = 10^{16.5}$ cm^{-2}, $b_{\rm CO} = 2.0$ km s^{-1}, $T_{\rm ex}^{\rm CO} = 300$ K, and a velocity offset from $z_{\rm GRB}$ of $\delta v_{\rm CO} = 30$ km s^{-1}. In all panels, $v = 0$ km s^{-1} corresponds to $z_{\rm GRB} = 3.0363$ and the orange dashed lines indicate blends between transitions.

the atomic transitions and that the bandheads show absorption to $\delta v \approx +1000$ km s^{-1}. At first glance, this suggests that the molecular gas has an extremely high velocity dispersion, a highly unlikely attribute for molecular gas. We interpret these unusual characteristics, instead, as the result of absorption from high rotational levels ($J > 10$) which have been populated by UV pumping from the GRB afterglow. This is analogous to the excitation of fine-structure levels in Fe^+, Si^+, and O^0 gas in other GRB galaxies (Prochaska et al. 2006; Vreeswijk et al. 2007). Such levels would be easily resolved with an echelle spectrum.

We have fitted the CO $A - X$ bandheads in the R1200 and B600 data with a series of models and find preferred values $N({\rm CO}) = 10^{16.5\pm0.3}$ cm^{-2}, $b_{\rm CO} = 2.0 \pm 0.3$ km s^{-1}, $T_{\rm ex}^{\rm CO} = 300^{+200}_{-70}$ K, and a velocity offset from $z_{\rm GRB}$ of $\delta v_{\rm CO} = 30 \pm 15$ km s^{-1} (Figure 4). The preferred values were found by minimizing the residuals between the data and the model for the 1–0, 2–0, and 4–0 CO bands simultaneously. Each model included all rotational levels up to $J = 25$, for a total of 225 CO transitions with transition data taken from fits to empirical data (Morton & Noreau 1994). We then visually compared the model prediction with the 6–0 and 8–0 CO bands seen in the B600 spectrum to assure consistency over a larger range of f-values; these bandheads set an upper limit of $N({\rm CO}) < 10^{17.2}$ cm^{-2}. Although a parameterization of the gas with an excitation temperature $\left(T_{\rm ex}^{\rm CO}\right)$ is not formally valid for a photon-pumped gas, we achieve a reasonable model.

We have analyzed the H_2 gas in a similar fashion. Because the Lyman–Werner lines are heavily saturated and blended, there is little sensitivity to the Doppler parameter $b_{\rm H_2}$. Adopting $b_{\rm H_2} = 3$ km s^{-1}, we varied $T_{\rm ex}^{\rm H_2}$ and $N_{\rm H_2}$ and compared these models against the data at $\lambda_{\rm rest} < 1100$ Å. Under the assumption that H_2 absorption dominates the opacity at $\lambda_{\rm obs} < 4200$ Å, we constrain $N_{\rm H_2} = 10^{21.2\pm0.2}$ cm^{-2} and $T_{\rm ex}^{\rm H_2} = 10$ to 300 K. Models with larger/smaller $N_{\rm H_2}$ values conflict with the observations. Our analysis sets an upper limit to the integrated molecular fraction $f_{\rm int}({\rm H_2}) < 0.13$, but we expect that the sightline is comprised of at least two clouds: one predominantly atomic and the other molecular.

Assuming solar relative abundances, the implied O column density is $N({\rm O}) > 10^{19.6}$ cm^{-2} for a Galactic equivalent column density $N_H > 10^{22.7}$ cm^{-2}. This metal column density implies that there should be significant absorption of soft X-rays by K-shells of O, Si, etc. In Figure 2(b), we present the X-ray spectrum and best-fit model of the *Swift* XRT data obtained 0.6–376 ks after the burst (Evans et al. 2008). We estimate an effective $N_{\rm H} = 10^{22.58\pm0.04}$ cm^{-2} and a photon index $\Gamma = 2.26 \pm 0.07$ for a power-law spectrum. Therefore, the metal column densities from analysis of both the UV and X-ray spectra are consistent. On the other hand, assuming the Galactic dust-to-metals ratio would give an extinction ($A_V > 10$ mag) inconsistent with the observations. We conclude that the gas has a much lower dust-to-metals ratio than Galactic (Galama & Wijers 2001; Watson et al. 2006).

4. DISCUSSION

The previous section described the physical properties of the ISM and the first clear detection of molecular gas in a GRB host galaxy. With an $A_V \approx 3.2$ mag, this represents a molecule-rich "translucent" sightline with effective UV shielding of CO (van Dishoeck & Black 1988). With $N({\rm CO}) \approx 10^{16.5}$ cm^{-2} and $N_{\rm H_2} \approx 10^{21.2}$ cm^{-2}, the abundance ratio of CO to H_2 is $\sim 2 \times 10^{-5}$. These values are consistent with detailed models of CO photodissociation in translucent environments (e.g., model T3 in van Dishoeck & Black 1988), and with the transition region between diffuse and dark clouds in the correlation plot of CO versus H_2 (Sheffer et al. 2008). Altogether, the gas

exhibits roughly solar metallicity, the dust has an extinction curve similar to that observed for Galactic molecular clouds, including a 2175 Å bump, and the CO/H_2 ratio is consistent with Galactic translucent clouds. We infer that at least some molecular clouds in the young universe have similar properties to those observed locally.

There are, however, two notable differences from the Galactic ISM. First, we observe a very large H I column density. This attribute is common to GRBs yet contrasts with the surface densities of local H I disks. While the formation of a molecular cloud requires a large dust column to absorb H_2-dissociating photons, the analysis of Krumholz et al. (2008) implies a 20 times lower column than observed. Perhaps the large $N_{\rm HI}$ value is a coincidence; these are routinely observed along GRB sightlines without molecules (Tumlinson et al. 2007) and our preferred model of the CO absorption suggests a velocity offset of $\delta v_{\rm CO} \approx +30$ km s^{-1} from the atomic metal lines. The second key difference is that we infer a much lower dust-to-metals ratio than Galactic regardless of whether that metal column is estimated from the UV or X-ray spectra. We interpret this difference as the result of a dust-poor, atomic phase that is spatially separated from the highly extinguished molecular cloud. Both phases of gas give rise to metal absorption (the profiles span the estimated 30 km s^{-1} offset; Figure 3) but we speculate that the atomic phase has a much lower dust-to-gas ratio.

Several lines of evidence argue against identifying this molecular cloud as the birthplace of the GRB progenitor. We detect strong absorption from C I and Mg I transitions indicating the gas lies greater than 100 pc from the GRB (Prochaska et al. 2006). If the molecular gas were within $\sim$ 10 pc of the afterglow, a significant column of H_2 would be excited to unbound states (Draine & Hao 2002). We have searched for such transitions at $\lambda_{\rm rest} > 1400$ Å and report no positive detections, setting an equivalent width limit $W_{\rm rest}(H_2^*) < 0.1$ Å (95% c.l.). We have searched for variability in the dust opacity, H I absorption, and in the equivalent widths of the metal-line transitions but detect none. The most plausible scenario, therefore, is that the gas lies beyond 100 pc from the afterglow, consistent with the estimate for photodissociation regions surrounding GRB progenitors (Whalen et al. 2008). We conclude that the molecular cloud identified in the afterglow spectrum of GRB 080607 arises in a neighboring, star-forming region.

This marks the first unambiguous detection of H_2 in a GRB sightline (among six intensively searched) and of CO (among $\sim$ 20 sightlines). Our results offer insight into the rarity of these detections. From our dust model, we estimate a rest-frame UV extinction of $A_{1100\text{Å}} \approx 8$ mag. If this afterglow were just 1 mag fainter, then the Lyman–Werner series could not have been detected. Similarly, the CO bandheads would not have been observable for the majority of GRBs. We conclude, therefore, that one requires an uncommonly luminous afterglow combined with a fortuitous path through an unrelated molecular cloud.

We contend further that a significant fraction of the subluminous optical bursts (also called "dark bursts;" Djorgovski et al. 2001; Jakobsson et al. 2005; Cenko et al. 2008) are events like GRB 080607 but with fainter intrinsic luminosity. An open and intriguing question is whether these dust-extinguished events correspond to unique host galaxies (e.g., intensely star-forming and dusty systems), or whether the hosts have properties similar to the general population and the variations along individual sightlines is geometrical (i.e., molecular clouds have small cross-section and are rarely intersected). A resolution of these two effects bears on the nature of molecular gas at high redshift including its distribution and relation to star formation. A multi-wavelength survey of the hosts, including searches for CO emission, may help distinguish between these scenarios.

Though rare, these high-z events enable studies at optical wavebands of rest-frame UV features that serve as powerful diagnostics of star-forming regions. This includes a precise redshift for follow-up observations, for example studies of CO in emission at millimeter wavelengths. Indeed, the CO 3–2 and 1–0 transitions lie at favorable observational frequencies. High-resolution spectroscopy of systems like GRB 080607 would also permit searches for additional molecules in the UV (e.g., C_2; Sonnentrucker et al. 2007). Finally, such systems easily satisfy the metal-strong DLA criteria of Herbert-Fort et al. (2006) and afford a special opportunity to study rare elements in the young universe. Assuming solar abundances, for example, we estimate that the Sn II λ1400, B II λ1362, and Pb II λ1433 transitions should all have rest-frame equivalent widths exceeding 50 mÅ.

J.X.P. is partially supported by NASA/*Swift* grant NNX07 AE94G, and an NSF CAREER grant (AST–0548180). A.V.F. is grateful for NSF grant AST–0607485 and the TABASGO Foundation. Most of the data presented herein were obtained at the W. M. Keck Observatory, which is operated as a scientific partnership among the California Institute of Technology, the University of California, and the National Aeronautics and Space Administration (NASA). KAIT has been supported primarily by donations from AutoScope Corp., Lick Observatory, the NSF, the Sylvia & Jim Kantzman Foundation, and the TABASGO Foundation. We acknowledge D. Welty for valuable discussions.

REFERENCES

Bloom, J. S., Starr, D. L., Blake, C. H., Skrutskie, M. F., & Falco, E. E. 2006, in ASP Conf. Ser. 351, Astronomical Data Analysis Software and Systems XV, ed. C. Gabriel, C. Arviset, D. Ponz, & S. Enrique (San Francisco, CA: ASP), 751
Butler, N. R., & Kocevski, D. 2007, ApJ, 663, 407
Butler, N. R., et al. 2006, ApJ, 652, 1390
Campana, S., et al. 2006, A&A, 449, 61
Cenko, S. B., et al. 2008, arXiv:0808.3983
Chen, H.-W., et al. 2008, arXiv:0809.2608
Chen, H.-W., Prochaska, J. X., Ramirez-Ruiz, E., Bloom, J. S., Dessauges-Zavadsky, M., & Foley, R. J. 2007, ApJ, 663, 420
Chevalier, R. A. 2004, in AIP Conf. Ser. 727, Gamma-Ray Bursts: 30 Years of Discovery ed. E. Fenimore & M. Galassi (New York: AIP), 355
Christensen, L., Hjorth, J., & Gorosabel, J. 2004, AAP, 425, 913
Dickey, J. M., & Lockman, F. J. 1990, ARA&A, 28, 215
Djorgovski, S. G., Frail, D. A., Kulkarni, S. R., Bloom, J. S., Odewahn, S. C., & Diercks, A. 2001, ApJ, 562, 654
Draine, B. T., & Hao, L. 2002, ApJ, 569, 780
Elíasdóttir, Á., et al. 2008, arXiv:0810.2897
Evans, P. A., Osborne, J. P., Burrows, D. N., & Barthelmy, S. D. 2008, GRB Coordinates Network, 7955, 1
Filippenko, A. V., Li, W. D., Treffers, R. R., & Modjaz, M. 2001, in ASP Conf. Ser. 246, IAU Colloq. 183: Small Telescope Astronomy on Global Scales, ed. B. Paczynski, W.-P. Chen, & C. Lemme (San Francisco, CA: ASP), 121
Fitzpatrick, E. L., & Massa, D. 1990, ApJS, 72, 163
Fruchter, A. S., et al. 2006, Nature, 441, 463
Fynbo, J. P. U., et al. 2006, A&A, 451, L47
Galama, T. J., & Wijers, R. A. M. J. 2001, ApJ, 549, L209
Herbert-Fort, S., Prochaska, J. X., Dessauges-Zavadsky, M., Ellison, S. L., Howk, J. C., Wolfe, A. M., & Prochter, G. E. 2006, PASP, 118, 1077
Hjorth, J., et al. 2003, Nature, 423, 847
Jakobsson, P., et al. 2005, MNRAS, 362, 245
Jakobsson, P., et al. 2006, A&A, 460, L13
Kann, D. A., Klose, S., & Zeh, A. 2006, ApJ, 641, 993
Kann, D. A., et al. 2007, arXiv:0712.2186
Krühler, T. 2008, ApJ, 685, 376

Krumholz, M. R., McKee, C. F., & Tumlinson, J. 2008, arXiv:0805.2947
Li, W., Filippenko, A. V., Chornock, R., & Jha, S. 2003, PASP, 115, 844
Mangano, V., et al. 2008, GRB Coordinates Network, 7847, 1
Morton, D. C., & Noreau, L. 1994, ApJS, 95, 301
Oke, J. B., et al. 1995, PASP, 107, 375
Perley, D. A., et al. 2008, ApJ, 672, 449
Prochaska, J. X., Chen, H.-W., & Bloom, J. S. 2006, ApJ, 648, 95
Prochaska, J. X., Chen, H.-W., Dessauges-Zavadsky, M., & Bloom, J. S. 2007, ApJ, 666, 267
Prochter, G. E., et al. 2006, ApJ, 648, L93
Ramirez-Ruiz, E., García-Segura, G., Salmonson, J. D., & Pérez-Rendón, B. 2005, ApJ, 631, 435
Savaglio, S., Fall, S. M., & Fiore, F. 2003, ApJ, 585, 638
Sheffer, Y., Rogers, M., Federman, S. R., Abel, N. P., Gredel, R., Lambert, D. L., & Shaw, G. 2008, ApJ, 687, 1075
Sonnentrucker, P., Welty, D. E., Thorburn, J. A., & York, D. G. 2007, ApJS, 168, 58
Srianand, R., Noterdaeme, P., Ledoux, C., & Petitjean, P. 2008, A&A, 482, L39
Stanek, K. Z., et al. 2003, ApJ, 591, L17
Tacconi, L. J., et al. 2006, ApJ, 640, 228
Tumlinson, J., Prochaska, J. X., Chen, H.-W., Dessauges-Zavadsky, M., & Bloom, J. S. 2007, ApJ, 668, 667
van Dishoeck, E. F., & Black, J. H. 1988, ApJ, 334, 771
Vreeswijk, P. M., et al. 2004, A&A, 419, 927
Vreeswijk, P. M., et al. 2007, A&A, 468, 83
Watson, D., et al. 2006, ApJ, 652, 1011
Whalen, D., Prochaska, J. X., Heger, A., & Tumlinson, J. 2008, ApJ, 682, 1114
Woosley, S. E., & Bloom, J. S. 2006, ARA&A, 44, 507
Woosley, S. E., & Heger, A. 2006, ApJ, 637, 914